Surface & Coatings Technology 268 (2015) 165–172

Contents lists available at ScienceDirect

Surface & Coatings Technology

journal homepage: www.elsevier.com/locate/surfcoat

Fireside corrosion degradation of HVOF thermal sprayed FeCrAl coating at 700–800 °C

T. Hussain [a,*], N.J. Simms [b], J.R. Nicholls [b], J.E. Oakey [b]

[a] Division of Materials, Mechanics and Structure, University of Nottingham, Nottingham, NG7 2RD, UK
[b] Institute for Energy & Resource Technology, Cranfield University, Bedfordshire, MK43 0AL, UK

ARTICLE INFO

Available online 7 February 2015

Keywords:
FeCrAl
HVOF
biomass/coal co-firing
Coal-ash corrosion
Fireside corrosion
superheater/reheater corrosion

ABSTRACT

To reduce the emissions of greenhouse gases, the power generation industry is increasingly moving towards higher operating steam temperatures (and pressures) and more efficient ultra super critical (USC) boilers. However, higher operating temperatures coupled with biomass derived fuel can lead to aggressive corrosion damage to the superheater reheater tubes. This paper presents a systematic evaluation of high velocity oxy fuel (HVOF) thermal sprayed FeCrAl coating onto a 9% Cr boiler steel. The coated samples were exposed in a series of laboratory-based fireside corrosion tests in simulated coal-biomass co-fired combustion gases for 1000 h at 700, 750 and 800 °C. The tests were carried out using the deposit-recoat test method to simulate the environment that anticipated from air-firing 20 wt.% cereal co-product (CCP) mixed with a UK coal. The exposures were carried out using a screening deposit containing Na_2SO_4, K_2SO_4 and Fe_2O_3 to produce alkali-iron tri-sulphates, which had been identified as being the principal cause of fireside corrosion on superheaters and reheaters in pulverized fuel power plants. Pre- and post-exposure dimensional metrology was used to quantify the metal damage in terms of metal loss distributions. The exposed samples were examined in an environmental scanning electron microscope (ESEM) to characterize the oxide scales and damage. At 700 °C, FeCrAl coating provided suitable protection (median metal damage of ~ 85 μm) to the steel substrate; however, at 750 °C, the median metal loss of the coating was ~260 μm and ~305 μm at 800 °C. Sulphur was detected at the coating-scale interface and an aluminium-rich mixed oxide formed at the outer scale and a chromium-rich mixed oxide formed in the inner layer. The concentration of aluminium in the coating depleted to ~ 6 at.% following the 1000 h exposure.

1. Introduction

Fireside corrosion (i.e., metal loss of heat exchangers due to chemical reactions with the combustion gases and deposits at high temperature) has been a life-limiting factor for the pulverised fuel power plants. Fireside corrosion can lead to tube failures through general metal loss or by formation of cracks, which can allow failure to occur by mechanical damage. These failures are difficult to repair and results in unscheduled plant shutdown. Fireside corrosion depends on the chemistry of the fuel and the deposit formed on the heat exchanger surfaces. When biomass is co-fired with coal, the combustion gases and the deposit chemistry change significantly altering the corrosion mechanisms [1]. Biomass contains higher levels of elements such as K and Cl and much less S compared to most coals [2,3]. The introduction of biomass can adversely affect the fireside corrosion of the heat exchangers. Biomass is considered a *carbon neutral* fuel and currently accounts for 70% of electricity generation from renewable sources [4]. Co-firing low levels of biomass in pulverised fuel power plants is an efficient way to introduce biomass fuels into the electricity generation industry. The pulverised coal fired power plants are much larger in capacity and more efficient than a dedicated biomass fired plant.

CO_2 and other greenhouse gases from the fossil fuel power plants are major contributors to global warming and resulting climate change. UK government has an ambitious target of reducing CO_2 emissions to 80% of their 1990 levels by 2050 [5]. The EU targets for 2020 and 2050 require major efficiency improvement of the pulverised fuel power plants. Reduction in CO_2 emissions from the pulverised coal-fired power plants can be achieved by increasing the operating temperatures and pressures of the steam system (hence increase in efficiency). Conventional pulverised fuel power plants operate at an efficiency of 36% [6,7], and 1% increase in absolute efficiency can result in as much as 3% reduction in CO_2 emissions [8]. To meet these national and EU targets, supercritical and ultra-supercritical power plants (~45% efficiency) are under development, where metal temperatures will be in excess of 650 °C. However, the increased metal temperatures will make the conventional alloys unsuitable due to creep and fireside corrosion limitations and a new generation of nickel-based alloys will be required. Alternatively, corrosion-resistant overlay coatings, which are cheaper than nickel-based substrates, can be used to provide suitable protection from the aggressive fireside corrosion. High velocity oxy-fuel (HVOF) thermal sprayed coatings can potentially protect the superheater and reheater

* Corresponding author. Tel.: +44 115 951 3795.
E-mail address: tanvir.hussain@nottingham.ac.uk (T. Hussain).

http://dx.doi.org/10.1016/j.surfcoat.2015.01.074
0257-8972/

components in power plants. The performance of nickel-based HVOF thermal sprayed coatings in boiler environment has been reported in literature [9–12], but so far no comprehensive study exists on iron-based HVOF thermal sprayed coatings. FeCrAl thermal sprayed coatings are of great interest to the power generation industry, as they are commercially cheaper than the nickel-based coatings and have similar co-efficient of thermal expansion.

The 9% Cr substrate used in this study is a ferritic martensitic steel, which is typically used at 650 °C in the various sections of the heat exchangers. Although, the material has good creep resistance, it suffers from steamside oxidation at that temperature. Fireside corrosion performance of this alloy is well established in various combustion environments in lab-scale accelerated tests from 600 to 750 °C [13–16]. In a power plant, the heat-exchanger materials have to survive around 100,000 h in operation. It is impractical to test the candidate materials and coatings for that long in a lab-scale-controlled environment test. There are two approaches to accelerate the tests: one is to increase the test temperature and run it for a shorter time period and the second is to use a more aggressive deposit by increasing the deposition fluxes. In this study, the fireside corrosion performance of FeCrAl HVOF thermal sprayed coating was tested with an aggressive screening deposit for 1000 h at the potential operating temperatures of the ultra supercritical (USC) power plant heat exchangers. A thermally sprayed protective coating for power plant applications need to address two distinctive issues: deposit induced corrosion performance of the coating and the coating–substrate interactions. The aim of this study was to focus on the corrosion performance of the coating.

The samples were exposed in simulated co-fired combustion gases at 700, 750 and 800 °C (metal temperatures anticipated in the USC boilers) for 1000 h. The combustion environment was based on co-firing a UK coal with a cereal co-product (CCP), and a synthetic deposit was used to assess the corrosion performance. The work was carried out using the deposit-recoat test method that has been developed for high-temperature corrosion [17–19]. Dimensional metrology has been used as the primary route to quantify the metal damage occurring due to the fireside corrosion. Following the exposure, the samples were examined in an environmental scanning electron microscope (ESEM) with energy dispersive x-ray (EDX) mapping to characterise the damage.

2. Experimental methods

2.1. Materials

FeCrAl coating was sprayed by Monitor Coatings Ltd. (Castolin Eutectic Group, Tyne and Wear, UK) using feedstock powder sourced from Sulzer Metco Inc. (USA). The nominal composition of the powder provided by the manufacturer was as follows: Al 5.9, C 0.029, Cr 21.7, Mn 0.76, P 0.013, S 0.005, Si 0.83 wt.% and Fe balance. The feedstock powder had a size range of +15–45 μm. The coatings were sprayed with Praxair TAFA JP5000 kerosene fuelled gun with optimised process parameters, which were developed as a part of a commercially funded project. The same optimised spraying parameters were used to manufacture samples for boiler probes and pilot-scale probes exposure (>10,000 h). The coating was sprayed onto a 9% Cr (T92) boiler steel, which is a candidate material for superheaters/reheaters in ultra-supercritical pulverised fuel power plants. The nominal composition of T92 was Ni 0.22, Cr 8.91, Mo 0.38, C 0.11, Si 0.37, Mn 0.45, P 0.009, S 0.002, V 0.2, Al <0.001, N 0.053, B 0.0037, Nb 0.06, W 1.53 wt% and Fe balance. Each fireside corrosion test sample was 10 mm in diameter and 10 mm long with chamfers on both ends to reduce the edge corrosion attack.

2.2. Exposure conditions

The test conditions were determined following a detailed investigation of gaseous environments that could be found around superheaters/reheaters in pulverised fuel power plants burning coal with biomass [16]. The test conditions for the simulated fireside corrosion tests were based on co-firing 80:20 wt.% of a typical UK coal (Daw Mill) with cereal co-product. The fuel compositions can be found in ref. [15]. The gas compositions produced from the fuel mix has been calculated using pilot and plant-scale validated models. The gas compositions have been simplified to their active components for the purpose of this study. The nominal gas compositions are shown in Table 1. The coatings were tested using a standard screening deposit mixture, which has been widely used in developing new alloys and coatings for the power generation industry [1,14,20–22]. The composition of the screening deposits is shown in Table 2. The mixture represents a composition of alkali-iron tri-sulphate that has been identified as being the major mechanism of fireside corrosion of superheaters/reheaters in pulverised fuel power plants [1,23,24]. Each test was run for 1000 h using the widely accepted deposit-recoat test method [17–19]. In total, three tests were conducted at 700, 750 and 800 °C, each lasting for 1000 h. The samples were cleaned before the exposure using isopropanol in an ultrasonic bath for 20 min. The cleaned samples were painted using a brush to apply a deposit loading of ~20 mg/cm^2. The screening deposit was mixed with isopropanol to make a thick slurry before painting. The test was cycled every 200 h and repainted with deposits to replenish any salts. The samples were weighed every 200 h with and without crucibles as well as before and after applying the deposits. As a part of the deposit recoat process, the samples and crucibles were weighted before and after each cycle. It provided a gravimetric check on their performance and enabled the calculation of traditional net specific mass change data.

2.3. Experimental setup

The simulated fireside corrosion tests were carried out in an alumina lined vertical controlled atmosphere furnace where pre-mixed gases were supplied through mass flow controllers to achieve the composition mentioned in Table 1. A schematic diagram of the test setup is shown in Fig. 1. The gas containing CO_2, O_2 and N_2 was supplied through a de-ionised water bottle to add the required amount of moisture. The exhaust gases were passed through a moisture trap and a scrubber solution (NaOH) before finally being released in the atmosphere. The test environment (e.g., gas composition and deposits) used in this study is well established and have been widely reported in literature. A number of articles published in the last 5 years reported the performance of various ferritic and (15Mo3,T22, T24) martensitic (T91, T92) alloys, austenitic steels (HR3C, 347HFG), nickel-based alloys (263, 718, 617) and various HVOF and plasma sprayed coatings (NiCrAlY, Ni50Cr, In625, etc.) in this test environment at various temperatures [12–14, 16,21,25].

2.4. Pre- and post-exposure measurements

The samples were vacuum impregnated using a low shrinkage cold mounting resin filled with ballotini (to further reduce shrinkage). The mounted samples were cross-sectioned, ground and polished to 1 μm surface finish using non-aqueous lubricants. Field emission ESEM (Philips XL30, Eindhoven, the Netherlands) was used to investigate the microstructure of the coating and the corrosion product. Backscattered electron imaging at 20 kV along with EDX (Oxford Instruments ISIS Link, Oxford, UK) was used to identify the elemental compositions on the cross-sections. EDX elemental mapping was also used to identify the distribution of the corrosion products in the coatings. To protect the scale and the corrosion product, the samples were mounted with

Table 1
Nominal gas compositions used in the fireside corrosion tests.

N_2 (vol.%)	O_2 (vol.%)	CO_2 (vol.%)	H_2O (vol.%)	SO_2 (vppm)	HCl (vppm)
73.8	4	14	8	1300	400

Table 2
Deposit composition (mol%) used in the fireside corrosion tests.

Na_2SO_4	K_2SO_4	Fe_2O_3
37.5	37.5	25

cold mounting resin, which is not conductive; hence, environmental scanning mode was used during the analysis. The porosity of the coating was measured on the polished cross-section of the BSE images using an image analysis software (ImageJ, National Institute of Health, USA). Three images each with an approximate area of 500 × 350 μm was used to measure the porosity and an average value was reported with standard error in mean.

Dimensional metrology of the samples before and after the tests formed a key part of this study. The method has been detailed in previous articles [12,16,21,25]. The same samples used for the ESEM analysis were used for the dimensional metrology resulting in an accurate representation of the data. In summary, the samples were measured to ± 1 μm using a micrometre prior to their exposure and were measured again following the 1000 h exposure using an image analyser connected to a microscope with a x–y coordinate stage. Post-exposure metrology was performed on prepared cross-sections of the samples, and co-ordinates from the post-exposure metrology were compared with the pre-exposure measurements to determine remaining metal thickness (metal loss). The measurement method is in accordance with the draft standard methods for high-temperature corrosion assessments [17–19].

3. Results

3.1. As-sprayed coating microstructure

Fig. 2a shows the as-sprayed microstructure of the FeCrAl coating onto the substrate. The coating shows well-bonded interface with the substrate without any sign of delamination. The nominal thickness of the coating was around 250 μm. The darker contrast particles at the coating-substrate interface were identified as embedded alumina (identified by the ESEM/EDX), as the substrate was grit blasted using alumina before coating deposition. The porosity of the coating measured on the cross-section images using the image analysis method was 2.6 ± 0.1%.Fig. 2b shows the higher magnification image of the coating microstructure. The microstructure contains semi-molten particle (spectrum 1: 9 at.% O, 12% Al, 20% Cr, 3% Si and Fe balance) and oxide inclusion (spectrum 2: 26 at.% O, 22% Al, 13% Cr, 2% Si and Fe balance). Inter-particle porosities can be identified in the micrograph. The composition of the semi-molten particle suggests little oxidation of the particle core during in-flight and the solidification process. The Al and Cr content of the coating were similar to those of the feedstock powder (5.9 wt.% Al and 21.7% Cr). The darker phase (spectrum 2) is due to in-flight oxidation of aluminium, which contained higher amount of Al and O than the coating matrix, due to in-flight oxidation of the Al. Aluminium has a higher affinity for oxidation out of all the elements present in the coating. Spectrum 3 shows a region which was molten during the spraying process, and the EDX spot analysis shows the following composition 12 at.% O, 11% Al, 19% Cr, 3% Si and Fe balance. The composition is similar to the composition at the core of the semi-molten particle with slightly more oxygen content. The samples were prepared with a non-aqueous oil-based lubricant, which has trace amount of Si.

3.2. Post-exposure coating microstructure

Fig. 3 shows the post-exposure microstructure of FeCrAl coating following 1000 h exposure in simulated co-fired combustion gases at 700, 750 and 800 °C. The microstructure of the coating at 700 °C shows a mixed layer of scale and deposits at the top. A two-layered deposit/scale morphology can be identified looking at the contrast of the BSE image. The particle–particle boundaries in the coating are clearly identifiable following the fireside corrosion tests. A line scan across the coating scale was performed to detect the levels of aluminium, chromium and oxygen in the coating exposed at 700 °C. The level of oxygen in the coating was low with spikes associated with oxidation at the inter-splat regions. It is interesting to note that the levels of iron in the coating varied to some extent, which corresponds to the levels of aluminium and chromium present in the coating. The regions, which are rich in aluminium showed a drop in the concentrations of iron in the line scan. The concentration of chromium increased towards the coating-scale and coating-substrate interface. Looking at the

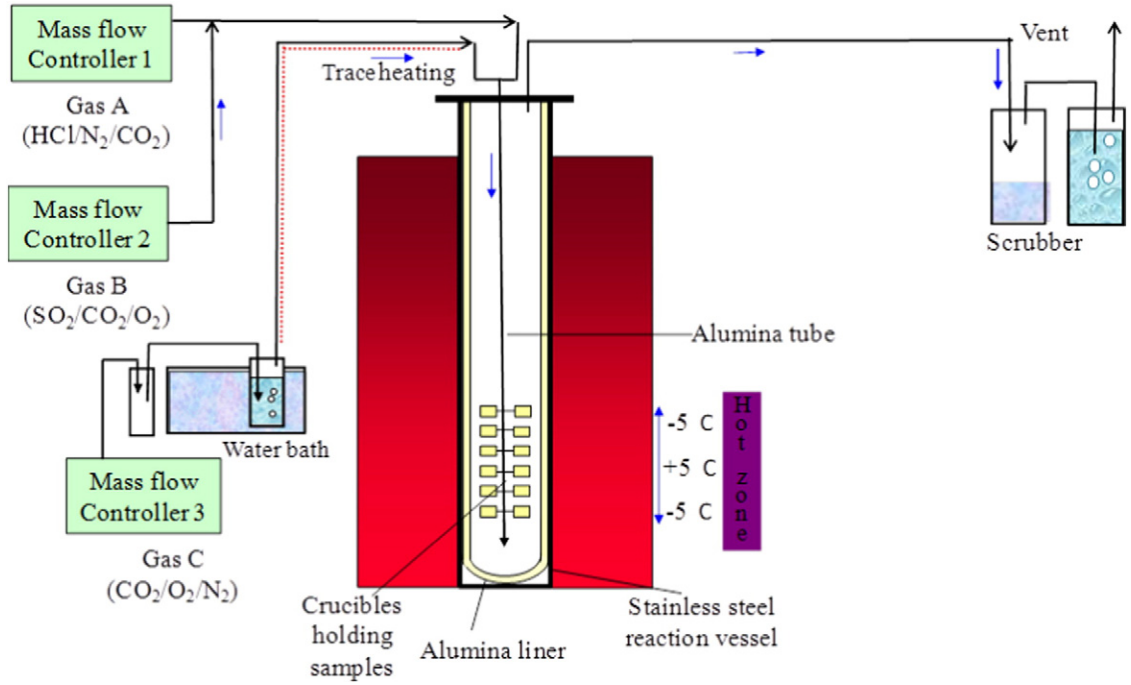

Fig. 1. Schematic diagram of a controlled environment fireside corrosion test setup.

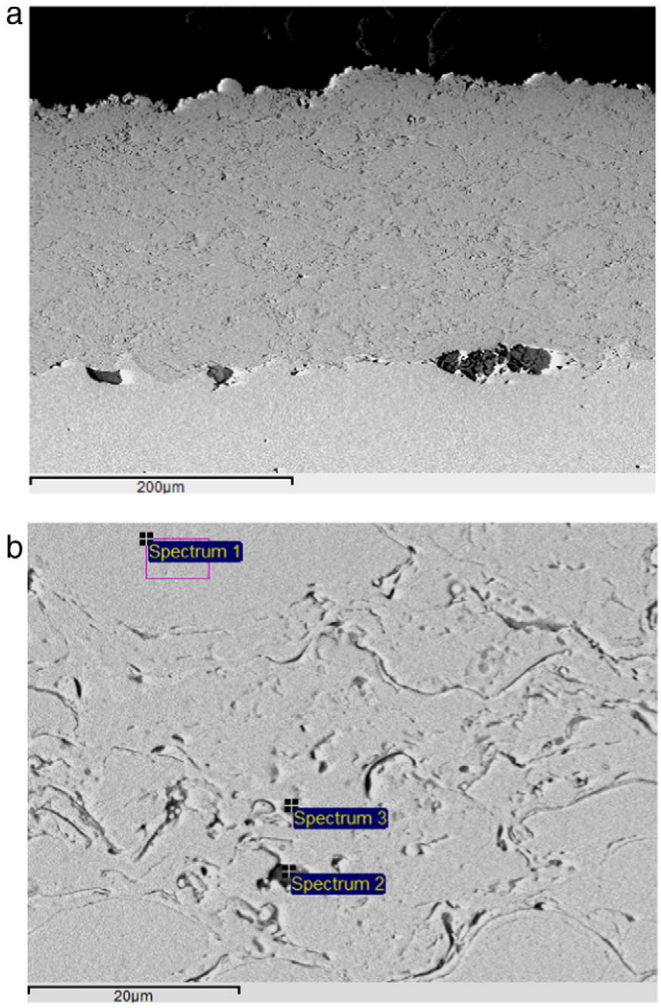

Fig. 2. BSE images of the (a) as-sprayed FeCrAl coating onto the substrate and (b) a higher magnification image showing detailed microstructural features. EDX spectra of the points are discussed in the text.

coating-scale interface, the inner region is rich is sulphur, which indicates sulphidation attack mechanism. The scale closer to the substrate (inner scale) has a higher concentration of chromium with small amount of aluminium, and the outer scale is rich in aluminium with small amount of chromium. Detailed EDX elemental maps of the oxides are shown in Fig. 4. The post-exposure microstructure of the FeCrAl coating exposed at 750 °C is shown in Fig. 3b. The coating suffered from a broad pitting type attack as can be seen from a reduction in thickness at the centre. The scale/deposit layer consisted of various elements from the deposit and a mixed oxide phase consisting of aluminium and chromium oxides. The coating exposed at 800 °C showed significant oxidation of the splats (the darker phases at the particle-particle boundaries). A large pitting type attack of the coating can also be identified in Fig. 3c (similar to the sample from 750 °C).

Fig. 4 shows a higher magnification image of the coating cross-section, which was exposed at 750 °C with detailed microstructural features. EDX spot analysis was performed at the centre of the splat and the inter-plat oxides. Compared to the as-sprayed coating microstructure (Fig. 2), the exposed coatings show thickening of the inter-splat oxides and a darker phase within the splats. The centre of the splat (spectrum 3) had the following composition (14 at.% O, 2% Na, 6% Al, 4% Si, 1% S, 16% Cr and Fe balance). The level of aluminium has depleted in the exposed coating from 11 to 12 at.% (as-sprayed) to 6 at.%, and the level of chromium has depleted from the as-sprayed coating level of 20 at.% to 16 at.%. The migration of aluminium and chromium towards the coating-scale boundary has resulted in this decrease in the bulk of the coating. It is promising that the coating following a 1000 h exposure was not fully depleted in aluminium. The darker spots within the splat were identified as an aluminium-rich phase with the following composition at spectrum 2 (14 at.% O, 1% Na, 16% Al, 4% Si, 1% S, 14% Cr and Fe balance). The levels of oxygen in spectrum 2 and 3 are the same, but the main difference is in the concentration of aluminium. This phase is possibly an intermetallic phase of Fe_3Al, which according to the Fe-Al phase diagram can form at the test temperatures. The inter-splat oxide at spectrum 1 has thickened following the 1000 h exposure and has the following composition (29 at.% O, 1% Na, 17% Al, 3% Si, 1% S, 15% Cr and Fe balance).

To identify the mode of corrosion attack on the FeCrAl coating, EDX elemental mapping was performed. As an example, Fig. 5 shows the elemental maps of the FeCrAl coating, which was exposed at 700 °C for 1000 h. Iron is found in the coating as well as in the deposit. A thin band of aluminium-rich mixed oxide was found at the outer edge of the coating (which can also be identified as the darker contrast region in the BSE image). Underneath this layer, a mixed chromium-rich oxide was detected from the elemental maps. Sulphur was detected in the chromium-rich mixed oxide layer, suggesting the scales were not protective to stop inward migration of sulphur in the tests.

Fig. 6 shows a higher magnification BSE image of the FeCrAl coating following exposure at 800 °C. Looking at the elemental map, a network of chromium-rich oxide developed around the initial splats (spectrum 2: 48 at.% O, 8% Al, 19% Cr, 1% Si, 23% Fe and 1% Na). EDX spot analysis was also performed at the inter-splat region, which had a darker contrast (spectrum 3: 50 at.% O, 14% Al, 13% Cr, 1% Si, 21% Fe and 1% Na). The smaller size of this phase makes it very difficult to identify it reliably using the EDX spot analysis. This oxide at the inter-splat boundary is predominantly a chromium-rich oxide network with small inclusions of aluminium oxide. The aluminium-rich phase appeared darker in contrast in the BSE image.

From the elemental maps, it can be seen that the chromium is enriched on the outside of the coating at the coating-scale interface. EDX spot analysis of spectrum 1 has the following composition: 56 at.% O, 7% Al, 19% Cr, 1% Si, 16% Fe and 1% Na. The composition suggests it is a chromium-rich mixed oxide with Na, which came from the deposit. Moreover, from the EDX maps it can be seen that an aluminium-rich mixed oxide has grown on top of the chromium-rich mixed oxide layer.

3.3. Measurements of metal damage through dimensional metrology

Mass change data are the most conventional and frequently reported method of observing metal oxidation and corrosion at high temperatures [26,27]. There are many well-known drawbacks of using mass change data, and hence it limits the use of mass change data in many practical situations, which also complicates its interpretation. However, the generation of mass change data is still part of the draft standards for high-temperature corrosion testing and provides a means to compare with the published literature. The "deposit-recoat" method used in this study generates the necessary mass change data on each recoat cycle, and Fig. 7 shows the specific net mass change data for FeCrAl coated samples, which were covered with deposits in simulated combustion gases. In general, higher net specific mass gain was observed with increasing the test temperature. It is should be noted that no decrease in mass change was noticed during the exposure for 1000 h, suggesting no scale or coating spallation occurred during the exposure of the samples.

Dimensional metrology provides the most reliable measurement of corrosion damage to materials at high temperature, as it produces a distribution of metal damage data for each exposed samples [28,29]. The results are plotted as change in metal vs cumulative probability according to the draft standards for high-temperature corrosion measurements [17,18]. Fig. 8 shows the metal damage vs cumulative probability of FeCrAl coatings exposed in simulated co-fired combustion gases with screening deposits at 700, 750 and 800 °C for 1000 h. The

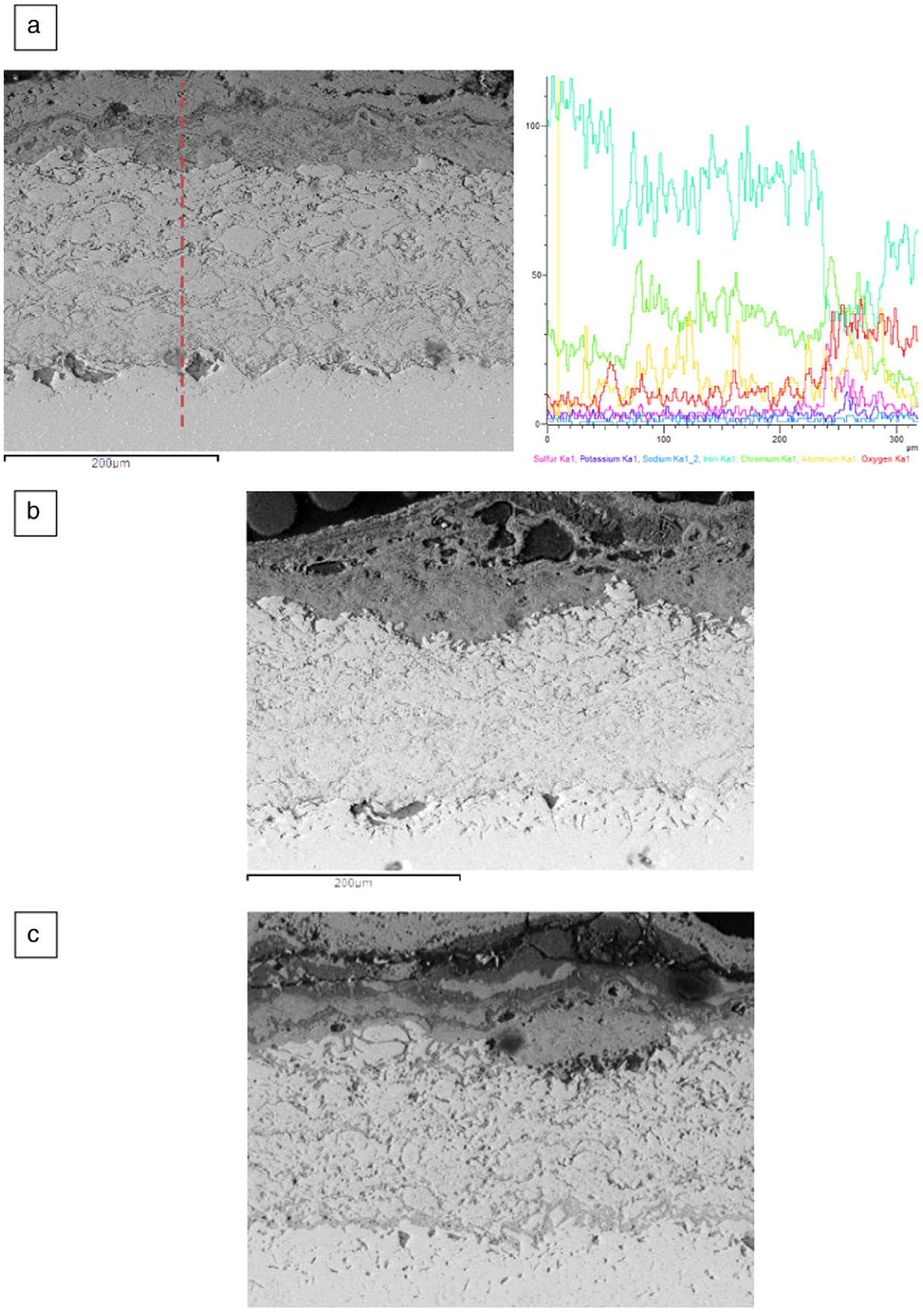

Fig. 3. BSE images of the FeCrAl coating following exposure in the simulated combustion gases with deposit at (a) 700 (with line scans showing elemental distribution), (b) 750 and (c) 800 °C.

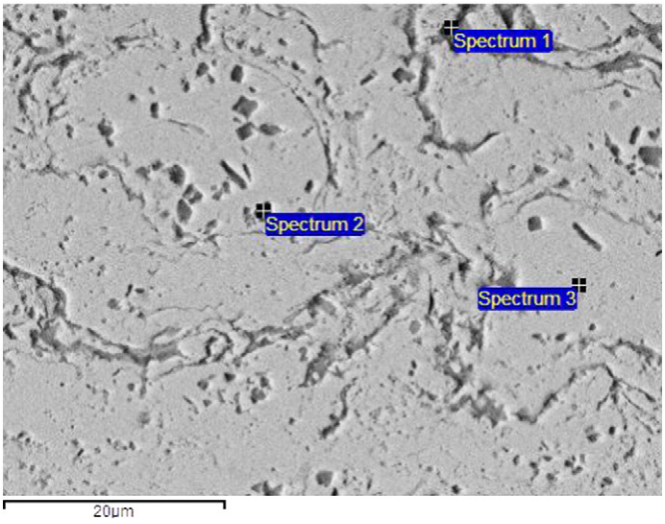

Fig. 4. BSE image showing inter-splat oxides and degradation of the FeCrAl coating after the exposure at 750 °C. EDX spectra of the points are discussed in the text.

least damage out of all three temperatures was observed at 700 °C with a median metal loss of ~85 μm. The median metal damage (i.e., metal damage at 50% cumulative probability) is a useful measure to compare coating performance. Fig. 9 shows the median metal losses of the coating at all three exposure temperatures with the minimum and maximum metal loss values as error bars. Typically, the thickness of the coating before the exposure was around 250 μm. At both 750 and 800 °C, the median metal damages were more than ~250 μm. The most aggressive damage was observed at 750 °C with a maximum metal damage of 770 μm. According to Fig. 8, 55% of the sample surface had no coating left after exposure at 750 °C (metal damage more than 250 μm). The sharp steps in the metal loss curves indicate non-uniform metal damage. For example at 750 °C, 10% of the sample surface suffered from a damage more than ~550 μm and 90% of the sample surface suffered from a damage more than ~57 μm. The sample surface after 1000 h exposure at 800 °C showed a median metal loss of ~300 μm. It should be noted that the screening deposit is an aggressive deposit that is used to accelerate superheaters/reheaters corrosion damage in laboratory exposures.

4. Discussion

Typically, metal damage to the alloys or coatings increases with increasing temperature, although the rate of damage depends on the kinetics. In this study, the damage to FeCrAl coating at 750 and 800 °C increased by a factor of ~3.5 times compared to that of 700° (comparing the median metal loss values). Traditional target corrosion values for superheater/reheater materials in conventional coal fired power plants are ~40–50 μm/1000 h. The metal loss values in this study are well in excess of those target values. However, it should be noted that the screening deposit used in this study is an aggressive deposit, which accelerates the corrosion used in laboratory corrosion tests. In service conditions, the flux of the alkali salts will be less due to clay minerals and ash in the deposits. For comparison, in similar combustion gases with a screening deposit, a bare T92 substrate at 700 °C shows a median metal loss of ~850 μm with a maximum metal loss of ~950 μm and a minimum metal loss of ~800 μm [16]. There is no doubt that the use of FeCrAl provided considerable protection to the substrate at 700 °C (e.g., the median metal loss of FeCrAl was ~85 μm). The corrosion damage to the coating is believed to be due to the formation of molten complex alkali-iron tri-sulphates. Possible series of reactions of forming alkali-iron tri-sulphates are [30]

$$SO_2 + 1/2O_2 \leftrightarrow SO_3 \quad (1)$$

$$Fe_2O_3 + 3SO_3 \leftrightarrow Fe_2(SO_4)_3 \quad (2)$$

$$3(Na/K)_2SO_4 + Fe_2(SO_4)_3 \leftrightarrow 2(Na/K)_3Fe(SO_4)_3 \quad (3)$$

The alkali-iron tri-sulphates melt at a much lower temperature than alkali-sulphates, with a minimum melting point of ~550 °C [30–33]. The deposit needs SO_3 to be stabilised at high temperatures. In this study,

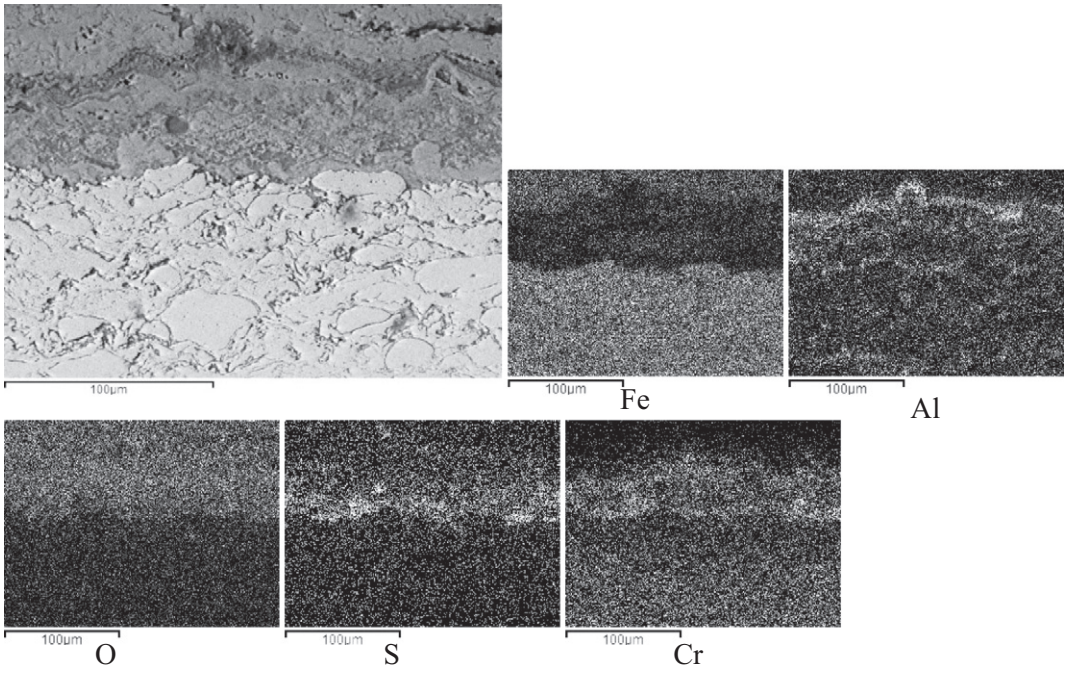

Fig. 5. BSE image and corresponding EDX elemental maps showing the FeCrAl coating after the exposure at 700 °C.

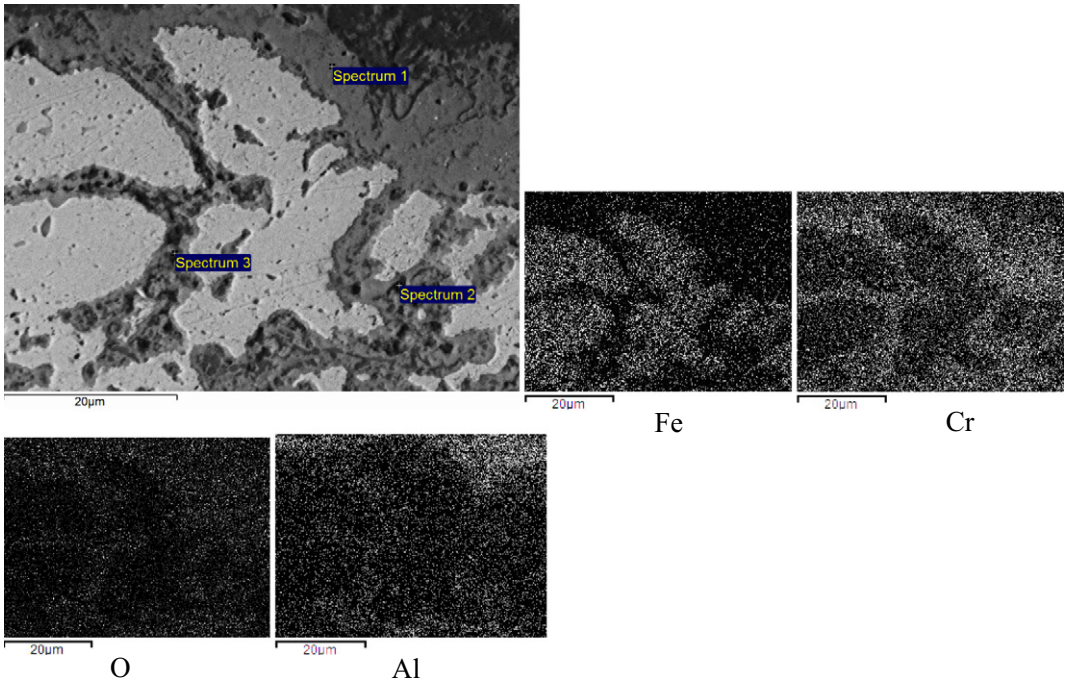

Fig. 6. Higher magnification BSE image showing individual splats and EDX maps of the FeCrAl coating after the exposure at 800 °C.

the test conditions were above this melting point and hence the deposits were molten.

In fireside corrosion, typically the austenitic steels show a characteristic *bell-shaped* curve, where the material damage increases with increasing temperature and after reaching a peak decreases with increasing temperature. In a previous study with the same combustion environment and the same screening deposits, the peak was found to be at around 650 °C. This was due to de-stabilisation of the molten complex alkali-iron tri-sulphates with increasing temperature [16]. It another study with HVOF sprayed FeCrAl coating, it was found that the median metal loss of at 650 °C under similar conditions was ~140 μm at 650 °C with a maximum damage of ~185 μm and a minimum damage of ~105 μm [12]. In this current study, the median corrosion damage of the FeCrAl coating at 700 °C was ~ 85 μm, which follows the decreasing trend of the so-called *bell-shaped* curve. However, above 700 °C, the corrosion damage increased rapidly with increasing temperature, suggesting a different corrosion mechanism is taking place, which is not related to the de-stabilisation of the deposits. It is believed that the oxidation damage is dominating over the corrosion damage beyond 700 °C, resulting in an overall change in degradation mechanisms. Similar behaviour was observed in nickel-based alloys (263, 617, 718), where a change in degradation mechanism occurred above 700 °C with significant internal damage [34].

FeCrAl coating has traditionally been used for high-temperature oxidation applications, and the published literature lacks information on the coating in fireside corrosion environments. FeCrAl alloys typically form protective α-Al_2O_3 at around 900 °C, but metastable γ-Al_2O_3 (sometimes θ and δ) sub-layers can be detected when exposed at lower temperatures [35]. The lowest amount of Al required to form an alumina layer is ~ 3.2 wt.% at around 900 °C in air [36]. Alloys with less than 3 wt.% Al usually form a three layered oxide layer consisting of an outer iron oxide, intermediate chromium oxide and an inner aluminium layer. The oxide growth involves transportation of ions through the oxide layer, which is controlled by diffusion mechanisms. During the migration mechanisms, metal ions diffuse from the oxide/metal interface to the

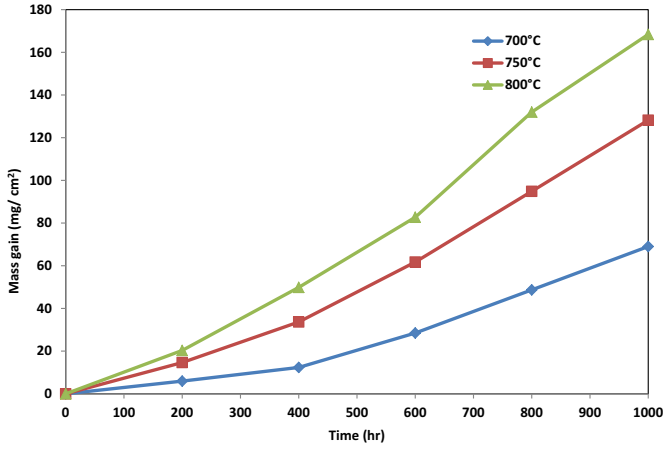

Fig. 7. Mass change data of the FeCrAl coated substrates following exposure in the simulated combustion gases with deposit at 700, 750 and 800 °C according to deposit-recoat method.

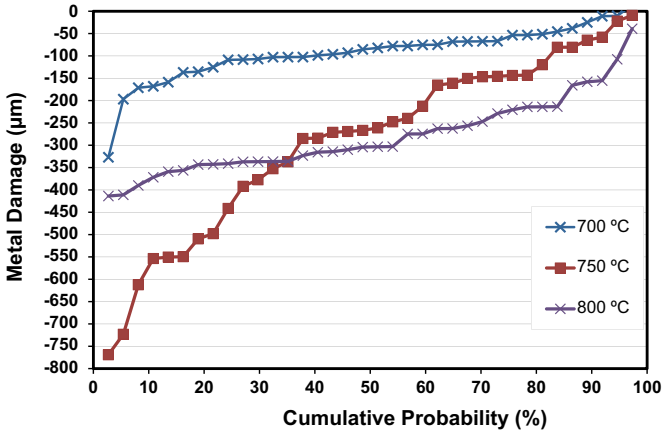

Fig. 8. Metal damage vs. cumulative probability of FeCrAl coating covered in deposits in simulated combustion gases after 1000 h at 700, 750 and 800 °C.

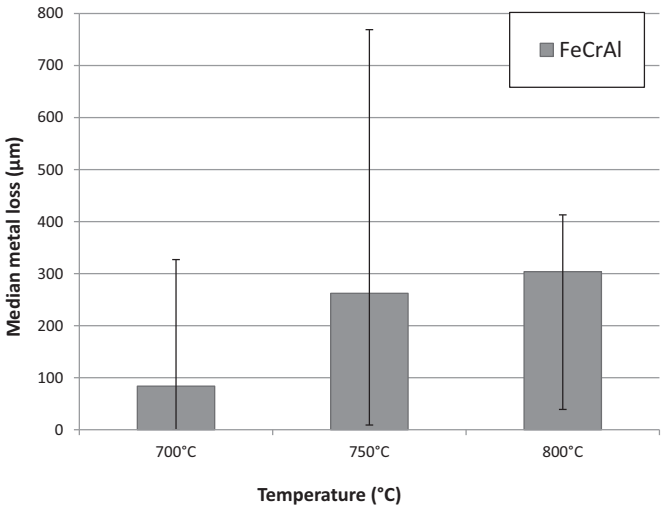

Fig. 9. Median metal loss of FeCrAl coatings covered in deposits in simulated combustion gases after 1000 h at 700, 750 and 800 °C with minimum and maximum values as error bars.

oxide/gas interface while the oxygen ions diffuse the opposite direction. The alumina oxide growth can be inward when it is predominating by oxygen diffusion or outwards when the diffusion of aluminium is faster through the layer. This mechanism is widely accepted for the wrought or cast alloys, but the complex nature of the HVOF sprayed coating, which contains oxides, voids and segregated phases, makes it very difficult to identify the mechanism. In this study, an outer mixed oxide layer rich in aluminium was formed in the test temperatures, and an inner mixed oxide layer rich in chromium with aluminium was formed. Sulphur was found underneath the chromium-rich layer, suggesting the mixed oxides were not protective or gas tight in nature. Also, the concentration of aluminium in the coating decreased during the 1000 h exposure. The average concentration of the as-sprayed aluminium coating was 11–12 at.%, which decreased to 6 at.% following the exposure. The decrease in aluminium concentration is due to migration of aluminium towards the coating-scale interface. Although this is above the threshold required to form protective alumina scale (at appropriate temperatures,) the gaseous environment with deposits was not favourable to form such an oxide scale—a mixed aluminium-rich oxide with other elements formed instead of the protective alumina.

Significant coating damage was observed at several places at the higher two test temperatures. The mass change data of the samples do not suggest any spallation during the 1000 h exposure, which indicated that the coatings suffered from gradual aggressive corrosion damage with time and eventually, the whole coating thickness was consumed at various sections.

5. Conclusions

The effect of simulated co-fired combustion gases on the fireside corrosion of the HVOF thermal sprayed FeCrAl coating has been investigated with a synthetic deposit for 1000 h at 700, 750 and 800 °C. The tests were conducted in line with deposit-recoat test method for high-temperature corrosion and dimensional metrology formed a critical part of this study. The samples were examined in an ESEM with EDX elemental mapping, and traditional mass change measurements were also performed. The following conclusions can be drawn from this study:

- The FeCrAl coating performed best at 700 °C (~85 μm median metal loss after 1000 h) but suffered from aggressive corrosion damage at 750 and 800 °C. Median metal losses of the coating were ~260 and ~305 μm at 750 and 800 °C, respectively. The coating in all three temperatures suffered from progressive metal losses with exposure time and no spallation of the coating was observed from the mass change data.
- The coating produced an aluminium-rich mixed outer oxide layer and a chromium-rich mixed inner oxide layer underneath the synthetic deposit in the simulated combustion gases. Sulphur was detected underneath the inner mixed oxide layer suggesting a sulphidation attack; however, no chlorine was detected at the coating-scale interface.
- The bulk concentration of aluminium within the coating following the 1000 h exposure decreased to 6 at.% (from as-sprayed 11–12 at.%). The inter-splat oxides in the coating consisted of chromium oxides with aluminium-rich phases. Aluminium in the coating acted as a reservoir during the exposure; however, no gas tight protective alumina layer was formed at the coating-scale interface.

Acknowledgments

The authors acknowledge the support of the EU FP7—Energy funded NextGenPower (Meeting the Materials and Manufacturing Challenge for Ultra High Efficiency PF Power Plants with CCS, ENERGY.2009.6.1.1) and the following companies: Doosan Babcock, Monitor Coatings, VUZ, E.ON Benelux, VTT, Skoda, Saarschmiede, TU–Darmstadt, Aubert & Duval and Goodwin Steel Castings.

References

[1] J. Stringer, I.G. Wright, Oxid. Met. 44 (1995) 265–308.
[2] M. Aho, A. Gil, R. Taipale, P. Vainikka, H. Vesala, Fuel 87 (2008) 58–69.
[3] H.P. Nielsen, L.L. Baxter, G. Sclippab, C. Morey, F.J. Frandsen, K. Dam-Johansen, Fuel 79 (2000) 131–139.
[4] A.A. Khan, W. de Jong, P.J. Jansens, H. Spliethoff, Fuel Process. Technol. 90 (2009) 21–50.
[5] J. Skea, P. Ekins, UKERC energy 2050 project; S3097:30, 2009.
[6] P. Dechamps, in: J. Lecomte-Beckers, M. Carton, F. Schubert, P.J. Ennis (Eds.), Materials for Advanced Power Engineering, Grafische Medien, Leige, Belgium, 2006, pp. 25–40.
[7] J.P. Shingledecker, I.G. Wright, in: J. Lecomte-Beckers, M. Carton, F. Schubert, P.J. Ennis (Eds.), Materials for Advanced Power Engineering, Grafische Medien, Leige, Belgium, 2006, pp. 107–119.
[8] J. Henry, G. Zhou, T. Ward, Mater. High Temp. 24 (2007) 249–258.
[9] N. Bala, H. Singh, S. Prakash, J. Therm. Spray Technol. 19 (2010) 110–118.
[10] N. Bala, H. Singh, S. Prakash, J. Karthikeyan, J. Therm. Spray Technol. 21 (2012) 144–158.
[11] S. Paul, M.D.F. Harvey, J. Therm. Spray Technol. 22 (2013) 316–327.
[12] T. Hussain, T. Dudziak, N.J. Simms, J.R. Nicholls, J. Therm. Spray Technol. (2013) 1–11.
[13] T. Hussain, A. Syed, N. Simms, Oxid. Met. (2013) 1–12.
[14] A.U. Syed, T. Hussain, N.J. Simms, J.E. Oakey, Mater. High Temp. 29 (2012) 219–228.
[15] A.U. Syed, N.J. Simms, J.E. Oakey, Fuel 101 (2012) 62–73.
[16] T. Hussain, A.U. Syed, N.J. Simms, Fuel 113 (2013) 787–797.
[17] EC project SMT3-CT95-2001, TESTCORR, ERA Technology, UK, 2000.
[18] Draft ISO Standard. ISO/TC 156 NWI 5092005, 2006.
[19] S.R.J. Saunders, in: H.J. Grabke, D.B. Meadowcroft (Eds.), Guidelines for Methods of Testing and Research in High Temperature Corrosion, The Institute of Metals, London, 1995, p. 85.
[20] N.J. Simms, P.J. Kilgallon, J.E. Oakey, Energy Mater. Mater. Sci. Eng. Syst. 2 (2007) 154–160.
[21] T. Hussain, N.J. Simms, J.R. Nicholls, Mater. Corros. 64 (2013) 1–9.
[22] N.J. Simms, in: J.E. Oakey (Ed.), Environmental Degradation of Boiler Components, Power Plant Life Management and Performance Improvement Woodhead Publishing, 2011, pp. 145–179.
[23] E. Raask, Mineral Impurities in Coal Combustion, Hemisphere Publishing Corporation, 1985.
[24] K. Natesan, A. Purohit, D.L. Rink, US Department of Energy Fossil Energy Conference, 2003.
[25] A.U. Syed, T. Hussain, N.J. Simms, J.E. Oakey, High Temperature Corrosion, Gordon Research Conference, New London, NH, 2011.
[26] D. Young, High Temperature Oxidation and Corrosion of Metals, Elsevier, 2008.
[27] N. Birks, G.H. Meier, F.S. Pettit, Introduction to the High Temperature Oxidation of Metals, Cambridge University Press, 2006.
[28] N.J. Simms, in: J. Lecomte-Beckers, M. Carton (Eds.), Materials for Advanced Power Engineering, Forschungszentrum, Julich, 2010.
[29] J.R. Nicholls, P. Hancock, in: A. Rapp Robert (Ed.), NACE, Houston, Tex, USA, 1983, pp. 198-210.
[30] J. Tomeczek, Corros. Sci. 49 (2007) 1862–1868.
[31] A. Hendry, D.J. Lees, Corros. Sci. 20 (1980) 383–404.
[32] C.J. Cain, W. Nelson, Trans. ASME 83 (1961) 468–474.
[33] D. Lindberg, R. Backman, P. Chartrand, J. Chem. Thermodyn. 39 (2007) 1001–1021.
[34] T. Hussain, N.J. Simms, J.E. Oakey, International Conference on Life Management and Maintenance for Power Plants- New Tools and Solutions, Helsinki- Stockholm, 2013.
[35] H. Josefsson, F. Liu, J.E. Svensson, M. Halvarsson, L.G. Johansson, Mater. Corros. 56 (2005) 801–805.
[36] J. Engkvist, U. Bexell, M. Grehk, M. Olsson, Mater. Corros. 60 (2009) 876–881.